ELSEVIER

Biochemical Pharmacology 63 (2002) 1739–1754

Biochemical Pharmacology

Glutamate–cysteine ligase modifier subunit: mouse *Gclm* gene structure and regulation by agents that cause oxidative stress

Willy A. Solis, Timothy P. Dalton, Matthew Z. Dieter, Sarah Freshwater, Judy M. Harrer, Lei He, Howard G. Shertzer, Daniel W. Nebert*,[1]

Department of Environmental Health, Center for Environmental Genetics, University of Cincinnati Medical Center, Cincinnati, OH 45267-0056, USA

Received 22 June 2001; accepted 6 February 2002

Abstract

Glutamate–cysteine ligase is a heterodimer comprising a modifier (GCLM) and a catalytic (GCLC) subunit. In mouse Hepa-1c1c7 hepatoma cell cultures, we found that *tert*-butylhydroquinone (tBHQ; 50 μM) induces the GCLM and GCLC mRNAs ~10- and ~2-fold, respectively, and that these increases primarily reflect *de novo* transcription. We determined that the mouse *Gclm* gene has seven exons, spanning 22.3 kb; all exons, intron–exon junctions, and 4.7 kb of 5′-flanking region were sequenced. By RNase protection analysis, we identified two major and several minor transcription start-site clusters over a 300-bp region. The *Gclm* 5′-flanking region is GC-rich and lacks a canonical TATA box. Transient and stable transfection studies, using luciferase reporter constructs containing incremental *Gclm* 5′-flanking deletions (4.7–0.5 kb), showed high basal activity but only modest (~2-fold) inducibility by tBHQ. The only candidate motif for oxidative stress regulation (in the 4.7-kb region we sequenced) is a putative inverted electrophile response element (EPRE) 9 bp upstream from the 5′-most transcription start-site. Site-directed mutagenesis of this −9 EPRE demonstrated minimal (30–40%) decreases in tBHQ induction and no effect on basal activity—suggesting that this EPRE might be necessary but not sufficient. The nuclear erythroid factor-2 (NEF2)-related factor-2 (NRF2) is known to transactivate *via* EPRE motifs. In the presence of co-transfected NRF cDNA expression vector, however, no increase in *Gclm* promoter activity was observed. Thus, the endogenous *Gclm* gene shows robust transcriptional activation by tBHQ in the intact Hepa-1 cell, but reporter constructs containing up to 4.7 kb of promoter (having only the one EPRE at −9) demonstrate a disappointing response, indicating that the major tBHQ-responsive regulatory element of the mouse *Gclm* gene must exist either further 5′- or 3′-ward of the 4.7-kb region studied.

Keywords: Glutamate–cysteine ligase; Glutathione; Oxidative stress; *tert*-Butylhydroquinone; Mouse *Gclm* gene regulation; Electrophile response element; NRF2; Promoter analysis

1. Introduction

Reduced glutathione (GSH) is the most abundant cellular thiol and plays a role in numerous detoxification, bioreduction, and conjugation reactions [1–3]. GSH is a tripeptide that is synthesized by sequential reactions: glutamate and cysteine are first ligated by glutamate–cysteine ligase (GCL) to form γ-glutamylcysteine in the rate-limiting step [1]; γ-glutamylcysteine is then joined to glycine by glutathione synthetase to form GSH.

The GCL holoenzyme is a heterodimer comprising a catalytic subunit (GCLC) and a modifier subunit (GCLM). Whereas GCLC itself is capable of synthesizing γ-glutamylcysteine, interaction with GCLM improves its catalytic properties by lowering the K_m for the substrate glutamate and modulating the negative feedback inhibition (K_i) by

* Corresponding author. Tel.: +1-513-558-4347; fax: +1-513-558-3562.
E-mail address: dan.nebert@uc.edu (D.W. Nebert).

[1] GenBank accession numbers AF149054, AF149055, AF149056, AF149057, AF149058, AF149059, AF149060, and AH009833.

Abbreviations: GCL, glutamate–cysteine ligase; *Gclm* and GCLM, the mouse gene and mRNA/enzyme, respectively, for the modifier subunit of GCL; *GCLM* and GCLM, the human (or rat) gene and mRNA/enzyme, respectively, for the modifier subunit of GCL; *Gclc* and GCLC, the mouse gene and mRNA/enzyme, respectively, for the catalytic subunit of GCL; *GCLC* and GCLC, the human (or rat) gene and mRNA/enzyme, respectively, for the catalytic subunit of GCL; *Hmox1* and HMOX1, the mouse heme oxygenase-1 gene and mRNA/enzyme, respectively; *Nqo1* and NQO1, the mouse NAD(P)H:quinone oxidoreductase-1 gene and mRNA/enzyme, respectively; SOD1, Cu^{2+}/Zn^{2+}-superoxide dismutase; GSH, reduced glutathione; tBHQ, *tert*-butylhydroquinone; BSO, buthionine sulfoximine; EPRE, electrophile response element; NRF2, the nuclear erythroid factor-2-related transcription factor; TATA box, the TATAAA motif found on average 28 bases upstream from the transcription initiation site; CMV, cytomegalovirus; SV40, simian virus-40.

0006-2952/02/$ – see front matter
PII: S0006-2952(02)00897-3

GSH [2,3]. Thus, it has been proposed that, under physiological conditions, GCLC would not function properly without its interaction with GCLM [4]. Elucidation of mammalian *GCLC* and *GCLM* gene regulation should, therefore, be helpful in understanding how the cell maintains GSH homeostasis and protection against oxidative stress.

To date, much attention has been given to regulation of the *GCLC* gene. GCLC mRNA levels are increased in response to various agents that cause oxidative stress or that deplete cellular GSH (*reviewed in* [3,5,6]). Furthermore, it has been shown that transcriptional activation by oxidants is mediated by transcription factors acting through three DNA motifs: EPRE (also known as antioxidant response element, ARE) [7], a 12-*O*-tetradecanoylphorbol-13-acetate (TPA) response element (TRE) [8–11], and an NFκB response element [12,13].

In contrast, much less is known about mammalian *GCLM* gene regulation. The rat GCLM mRNA increases in response to oxidative stress conditions, and this effect is mediated through both transcriptional and post-transcriptional mechanisms [14]. However, these studies have not clearly identified the *cis* elements mediating transcriptional response of the *GCLM* gene. There have been efforts to understand the function of a putative functional inverted EPRE found in the 5′-flanking region of the human *GCLM* [15,16], mouse *Gclm* [17], and rat *GCLM* [18] genes.

The EPRE motif is a DNA consensus sequence found in the 5′-flanking regions of several phase II drug-detoxifying enzymes [19,20]. To date, there is limited evidence about the identity of the proteins that bind to this response element. The ''cap-'n'-collar'' NEF2 p45-related factor-2 (NRF2) [21] has been shown to be an essential member of the EPRE complex, however, binding to this motif in response to increased intracellular oxidative stress [22–26]. Based on these findings, one research group has implicated the putative functional inverted EPRE motif in the human *GCLM* proximal 5′-flanking region as an important enhancer for this gene [27]. On the other hand, another group has found this EPRE to be unnecessary for *GCLM* induction [28]. This controversy may in part be due to the nature of the *GCLM* 5′-flanking region, which lacks a TATA box and is very GC-rich [15–18].

As a step toward elucidating the transcriptional mechanisms regulating expression of the mammalian *GCLM* gene, we have cloned and characterized the intron/exon structure of the mouse *Gclm* gene. We have also characterized the transcriptional induction of *Gclm* in mouse Hepa1c1c7 (Hepa-1) hepatoma cells, identified the *Gclm* transcription start-sites, and designed 5′-flanking constructs to search for functional enhancer regions. Using this information, we show that the transfected *Gclm* 5′-flanking constructs and progressive deletions (from 4.7 to 0.5 kb), support high-level basal transcription with barely measurable responses to tBHQ and other inducers of oxidative stress. Finally, the contribution of the putative functional inverted EPRE motif is examined in transient transfections by site-directed mutagenesis and by transactivation with a NRF2 cDNA expression vector.

2. Materials and methods

2.1. Reagents

Diethylmaleate and tBHQ were purchased from Sigma–Aldrich. RNase A and T1 RNase were bought from Roche Molecular Biochemicals. SP6, T7 and T3 polymerases were purchased from New England Biolabs.

2.2. Cell culture and treatments

Hepa-1 cells [29] were cultured in Dulbecco's modified Eagle medium (DMEM) supplemented with 5% fetal bovine serum. Cells during logarithmic growth phase were treated with 1000× concentrated stocks of tBHQ dissolved in DMSO, by direct addition to medium. The highest DMSO concentrations used (0.1%) did not affect gene expression in these cell cultures. As a means to generate oxidative stress in the intact animal [30], diethylmaleate (5 mmol/kg) was given intraperitoneally to three 129/SVJ male mice (age 6 weeks), and hepatic total RNA was prepared 24 hr later.

2.3. Hybridization probes

Antisense cRNA probes were synthesized from cDNAs using SP6, T7 or T3 polymerase [31,32]. Creation of cDNA vectors containing the *Hmox1*, *Sod1*, and *Nqo1* genes have been previously described [33,34]. Templates for the GCLM and GCLC probes were derived from partial cDNAs prepared by reverse transcriptase–polymerase chain reaction (RT–PCR) of total RNA from tBHQ-treated Hepa-1 cells. The primers for GCLM and GCLC have been described elsewhere [35]. Amplified cDNA fragments were cloned into Bluescript SK^- (Stratagene) and sequenced to verify authenticity.

2.4. RNA preparation and analysis

Total RNA was extracted, size-separated and blotted on nylon membranes, and specific transcripts were measured, as previously described [32,36,37]. Transcripts were quantitated, using a Storm Phosphorimager (Molecular Dynamics).

2.5. RNase protection analysis

Total RNA was isolated [36] from livers of diethylmaleate-treated 129/SVJ mice and total RNA from tBHQ-treated Hepa-1 cell cultures. The RNase protection assay was performed essentially as described [38–40]. Digests

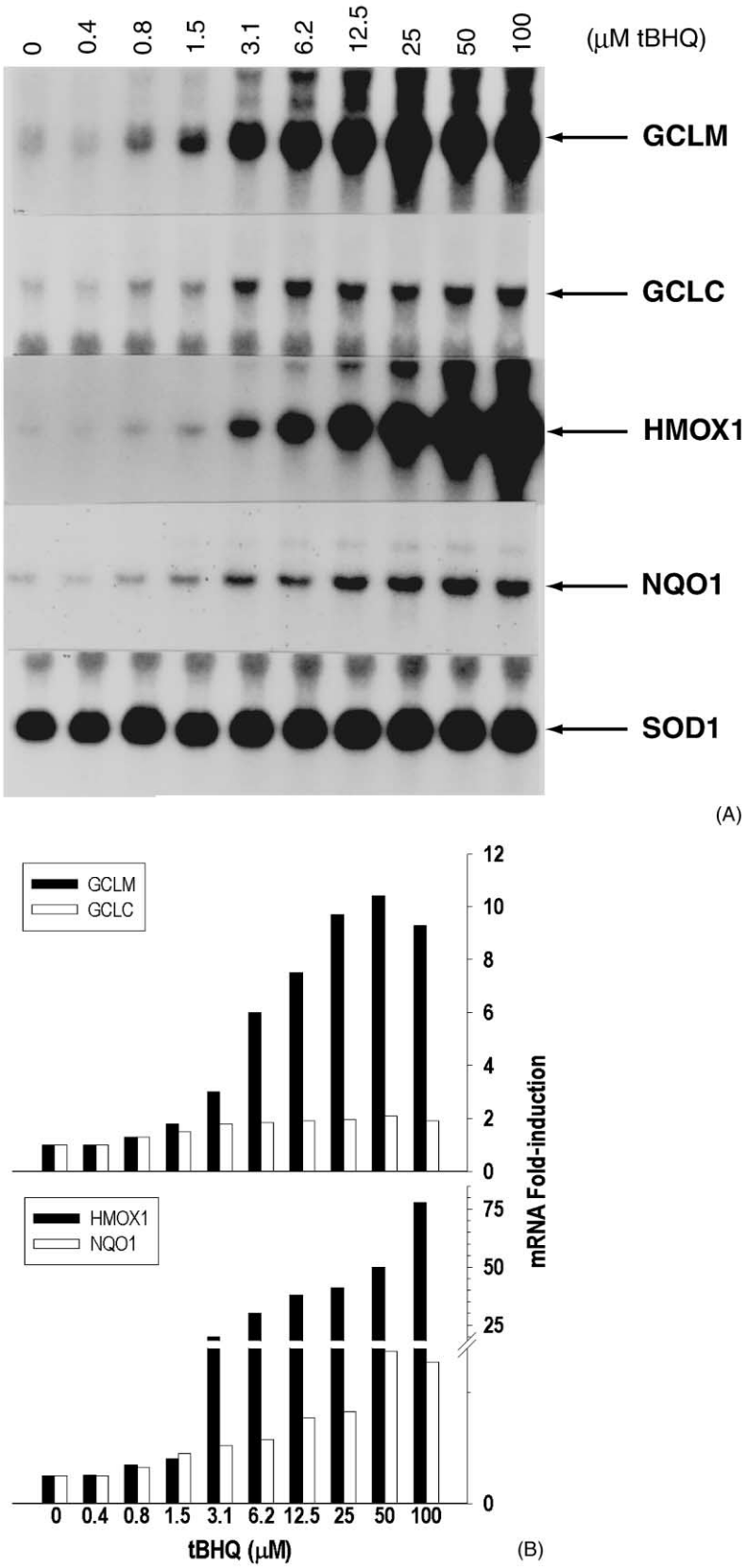

Fig. 1. Induction of GCLM, GCLC, HMOX1 and NQO1 mRNA by varying concentrations of tBHQ in mouse Hepa-1 cells. Treatment with tBHQ was 8 hr. The Northern blots (A) were semi-quantified by phosphorimager analysis (B), with SOD1 mRNA as the RNA-loading control for each lane. Note the differences in scale for fold-induction on the ordinate in (B).

contained 0.50–4.5 μg of RNase A and 24 Egami U of RNase T1. The hybridization temperature was 60°. Probes for hybridization extended from a *Sac* II site ~270 bp 3′ from transcription start-site cluster I to *Blp* I, *Stu* I and *Pst* I sites (0.5, 0.6, and 1.5 kb, respectively). The probes were judged by phosphorimager analysis to be >95% full-length. All three probe products identified the same two transcription start-site clusters. The approximate sizes of the protected transcripts were determined, using low-molecular weight RNA standards (Life Technologies) that were end-labeled with ^{32}P. These, in turn, were used to calibrate a DNA sequence ladder and adjust for the difference in mobility between DNA and RNA.

2.6. Isolation and sequencing of the Gclm gene

Overlapping clones containing the *Gclm* gene were isolated from a λ-phage genomic library, derived from the 129/SVJ mice (Stratagene). The library was screened using a random ^{32}P-labeled probe of the GCLM cDNA [41]. Individual λ-phage DNA clones were isolated using λ sorb (Promega), excised using *Not* I or *Sal* I, and cloned into Bluescript. Primers were designed for sequencing, using a GCLM full-length cDNA prepared by RT–PCR from mouse liver total RNA. Sequencing of our full-length mouse cDNA, all intron–exon junctions, and 4.7 kb of the *Gclm* promoter was performed by the University of Cincinnati DNA Core.

2.7. Construction of reporter plasmids

A segment of *Gclm* 5′-flanking region (4.7 kb) was cloned into the *Kpn* I and *Sac* I sites of the PGL3 Basic luciferase reporter gene (Promega). Using restriction endonuclease digests and blunt-end ligations, we generated the desired 3′-ward deletions. Two additional constructs, *p0.5GclmMutALUC* (MutA) and *p0.5GclmMutBLUC* (MutB), were generated—in which the putative inverted EPRE motif was mutated, using the Quick Change site-directed mutagenesis kit from Stratagene. The following sets of primers were used for this purpose:

wild-type A [5′-AGGTTTCTGCTTAGTCATTGTCTTCC-AGGAAACAGC-3′]
MutA1 [5′-AGGTTTCTGCTTAGT**AC**TTGTCTTCCAGG-AAACAGC-3′]
MutA2 [5′-GCTGTTTCCTGGAAGACAA**GT**ACTAAGC-AGAAACCT-3′]
wild-type B [5′-TCTCGGGTGAGGTTTCTGCTTAGTC-ATTGTCTTCCAGGAAACAGC-3′]
MutB1 [5′-TCTCGGGTGAGGTTTCT**AA**TTAGTC-ATTGTCTTCCAGGAAACAGC-3′]
MutB2 [5′-GCTGTTTCCTGGAAGACAATGACTAA**TT**AGAAACCTCACCCGAGA-3′]

The *EPREluc* reporter plasmid contains the mouse *Gsta1* EPRE enhancer region (−754 to −714) [42], as

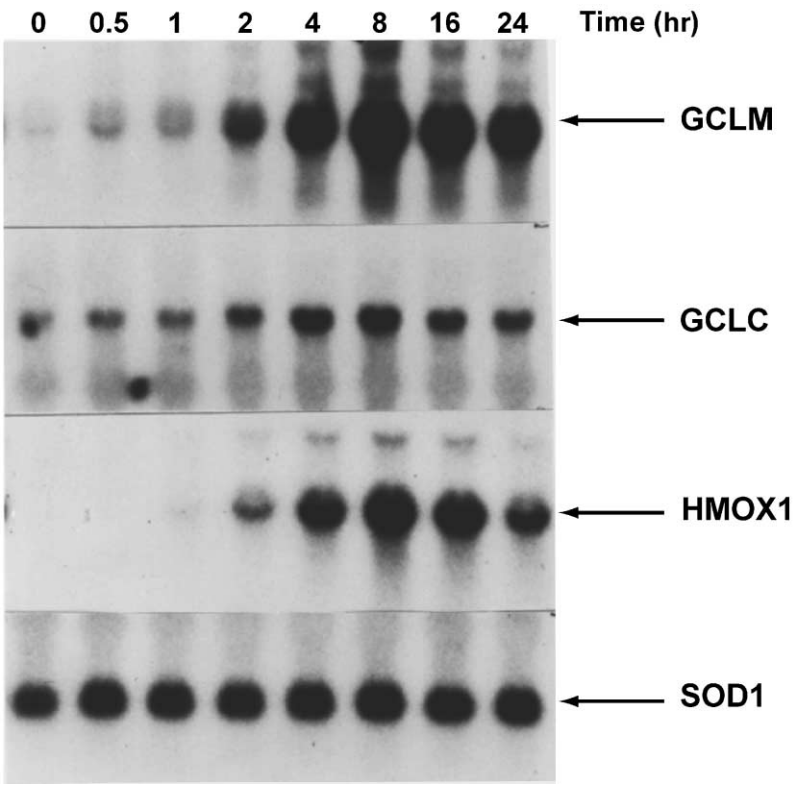

Fig. 2. Induction of GCLM, GCLC, and HMOX1 mRNA by 50 μM tBHQ as a function of time. Again, SOD1 mRNA was used as the RNA-loading control.

previously described [43]. The NRF2 expression plasmid has been described [44,45].

2.8. Cell transfections

Transfections were performed using the calcium phosphate precipitation method [46], or Lipofectamine (Life Technologies) using the manufacturer's protocol. Transient transfections contained a constant amount of plasmid DNA—which consisted of the reporter construct being tested, a CMV-β-galactosidase internal control plasmid (Promega), and Bluescript (Stratagene) as carrier. Stable transfections were prepared, using the reporter construct being tested and a CMV-driven β-galactosidase–neomycin phosphotransferase fusion gene (*βGeo*) plasmid. Cells were transfected for 12 hr, and then washed with PBS; after an additional 24 hr, selection medium containing geneticin (G418; Life Technologies) was added (at a concentration of 200 μg/mL), and selection continued for 14 days. G418-resistant clones were then harvested by trypsinization and pooled. Before experiments, the pooled stably transfected cells were incubated in G418-free culture medium for 48 hr.

2.9. Nuclear run-on transcription analysis and assay of oxidized (GS–SG), reduced (GSH) glutathione

These studies were performed as previously described [32,47].

3. Results

3.1. Accumulation of GCLM mRNA following tBHQ treatment

tBHQ-treated Hepa-1 cells exhibited a dose-dependent increase in GCLM mRNA (Fig. 1). Treatment with 50 μM

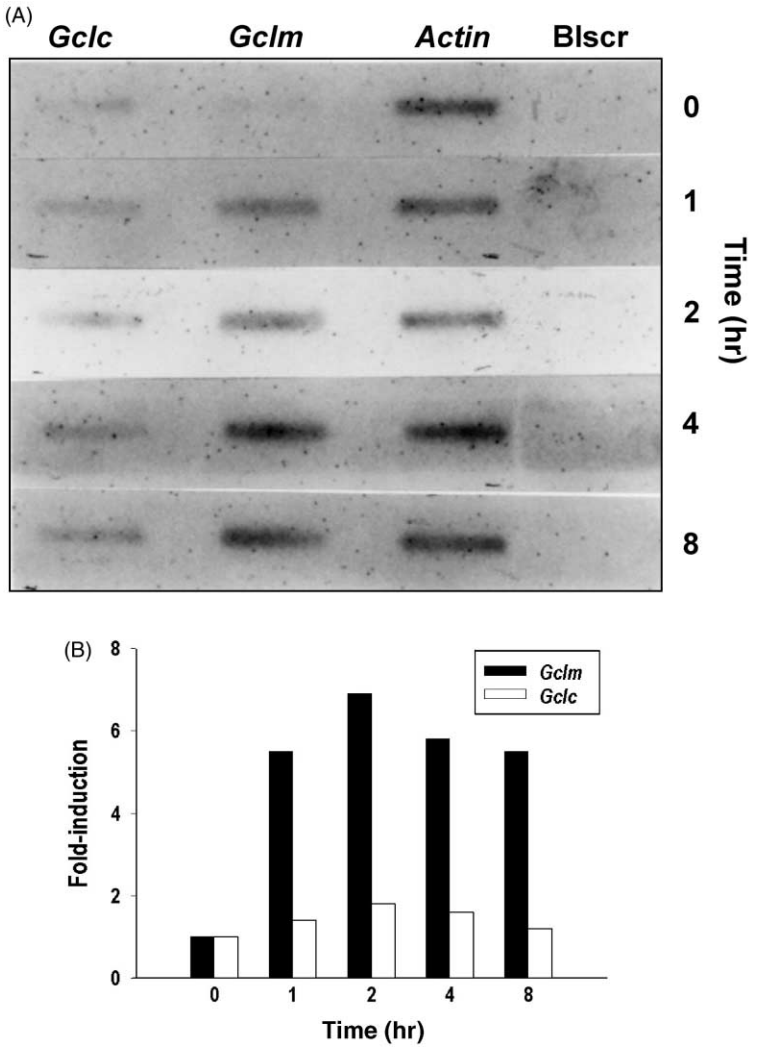

Fig. 3. Transcription run-on experiments with the mouse *Gclc* and *Gclm* genes. Hepa-1 cells were treated with tBHQ (50 μM) or vehicle (DMSO) alone for the indicated times. Visualization by autoradiography (A) was semi-quantified by phosphorimager analysis (B). Results were normalized to actin transcription controls and represent the average of two experiments. Blscr, Bluescript negative control.

tBHQ resulted in maximal (~10-fold) increases in GCLM mRNA. On the other hand, only modest increases (~2-fold) in GCLC mRNA were found. Treatment of cells with 50 μM tBHQ for as long as 24 hr did not cause cell toxicity, as judged by trypan blue exclusion (data not shown). The rates of mRNA accumulation for the *Gclm*, *Gclc*, *Hmox1*, and *Nqo1* genes were compared as a function of tBHQ concentration during an 8-hr treatment period (Fig. 1); although the relative levels of mRNA varied, the mRNAs for all four oxidative stress–responsive genes accumulated with similar dose–response relationships. Holding the tBHQ concentration constant (50 μM) and varying the time of tBHQ treatment (Fig. 2), we also found similar kinetics of mRNA accumulation for the *Gclm*, *Gclc*, and *Hmox1* genes. These data suggest that tBHQ-mediated oxidative stress induction of these four genes may involve the same DNA motifs and transcription factors binding to these motifs.

3.2. Comparison of five agents causing oxidative stress

The relative rates of accumulation of these mRNAs were compared—following treatment with varying concentrations of tBHQ, hydrogen peroxide, menadione, cadmium, or arsenite—in the mouse Hepa-1 cell line, in the SV40 large T antigen-transformed fetal hepatocyte *ch/ch* cell line [48], and in the L929 cell line. The five agents were not remarkably different in the induction of these four mRNAs (data not shown), so we chose to do all the remaining studies with tBHQ. tBHQ is known to generate reactive oxygen species and has been widely used as a prototypic inducer of oxidative stress–responsive genes, especially in cell culture [49].

3.3. Relationship between induced mRNA accumulation and gene transcription

Is the accumulation of tBHQ-induced GCLM and GCLC mRNA due to an enhanced rate of transcription, increases in mRNA stabilization, or some combination of both? Nuclear run-on transcription experiments (Fig. 3) confirmed that the fold-induction for both mRNAs reflected primarily increases in transcription rates. Run-on transcription in two experiments increased 5- to 7-fold for the *Gclm* gene and, maximally, about 2-fold for the *Gclc* gene. Using actinomycin D, we also measured the decay of GCLM mRNA with and without tBHQ treatment. In all cases we found the half-life of GCLM mRNA to be greater than 8 hr, and no significant differences in half-lives were seen between tBHQ-induced and constitutive GCLM mRNA samples (data not shown).

3.4. GCLM mRNA levels during GSH depletion

GSH levels are known to decline as a result of oxidative stress [1–3]. Hepa-1 cells were, therefore, treated with buthionine sulfoximine (BSO), an enzymatic inhibitor of GCL [1], in order to deplete GSH levels. As previously reported [50], treatment of Hepa-1 cells with 10 μM BSO resulted in a time-dependent plunge in GSH levels (Fig. 4). Following 16 and 24 hr of BSO treatment, GSH levels fell to 40 and 20% of control levels, respectively, and GS–SG levels rose from 1 to 10%. Despite this decrease in GSH and increase in GS–SG, however, no increases in GCLM or GCLC mRNA were seen (Fig. 4). These data suggest that the absolute level of GSH or GS–SG in the cell is not a signal for the accumulation of GCLM or GCLC mRNA, or that the intracellular localization of GS–SG or whatever GSH still exists might be able to compensate so that the *Gclm* and *Gclc* genes are not activated.

3.5. Isolation of Gclm genomic clones

Using a mouse GCLM partial cDNA [41] generated by PCR, we screened a λ-phage genomic library and obtained

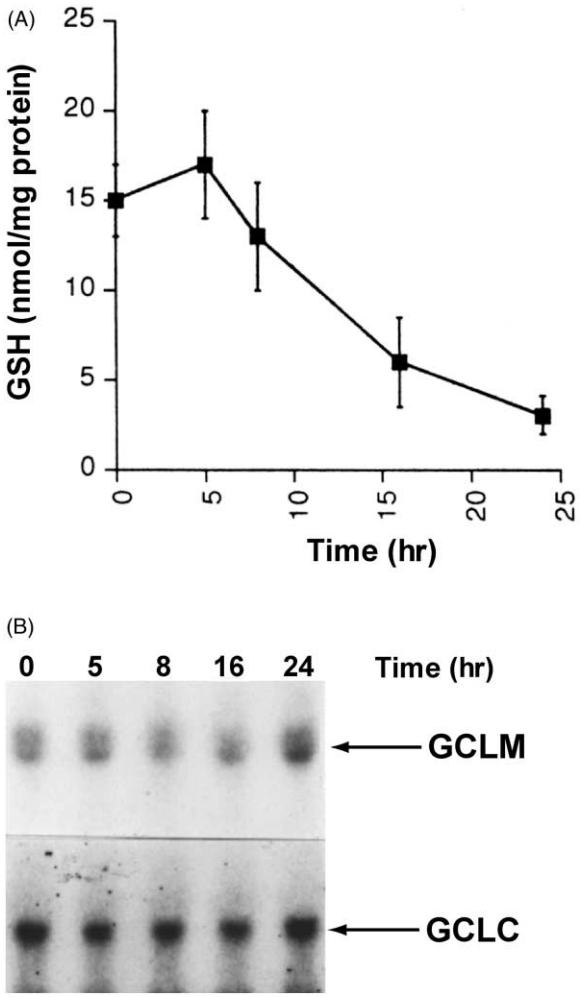

Fig. 4. Lack of an effect of GSH depletion on GCLM or GCLC mRNA concentrations. Hepa-1 cells were treated with 10 μM BSO and harvested at the indicated times. GSH levels were determined (means ± SD for three independent experiments) (A), and GCLM and GCLC mRNA levels were estimated by Northern blot analysis (B).

six overlapping clones. The clones exhibited compatible restriction digestion patterns, indicating that all six clones were derived from a single gene (data not shown). Using mouse GCLM cDNA primers, we determined that the *Gclm* gene contains seven exons and spans ~22.3 kb (Fig. 5). The approximate sizes of the *Gclm* introns were determined by PCR of the appropriate λ-phage clones, and all intron–exon boundaries displayed the consensus sequence for donor (GT) and acceptor (AG) splice sites (Fig. 5B). Thirty bases into each intron should provide sufficient sequence for primer design—in order for anyone to search in the future for DNA sequence variants within the coding region of the *Gclm* gene from any inbred mouse strain or other genetic variant.

The polyadenylation site that we found in exon 7 adds an additional 440 bp to the 3′ untranslated region, as compared with that reported by Reid *et al.* [41] who used oligo(dT) to prime for cloning the cDNA and apparently primed from a stretch of adenines in the 3′ untranslated region that turns out to be further 5′-ward than the actual polyadenylation site and poly(A) tract. This additional 440 bp is also consistent with the 1.9-kb band found for GCLM mRNA on Northern blots.

3.6. Determination of *Gclm* transcription start sites

Sequences 5′-ward and 3′-ward of the translation start-site cluster I in the *Gclm* gene are extremely GC-rich (Fig. 6A), and this might lead to the formation of stable secondary structures—thereby impeding normal extension by reverse transcriptase. For this reason, we mapped the transcription start sites using RNase protection analysis. After hybridization and digestion with RNase, we determined the sizes of the protected fragments, which correspond in length to the protected 5′-untranslated regions of the GCLM mRNA (Fig. 6B).

RNA samples isolated from the liver of diethylmaleate-treated 129/SVJ mice, as well as from tBHQ-treated Hepa-1 cells, were incubated with a riboprobe synthesized from 129/SVJ genomic DNA fragments. This approach was

(A)

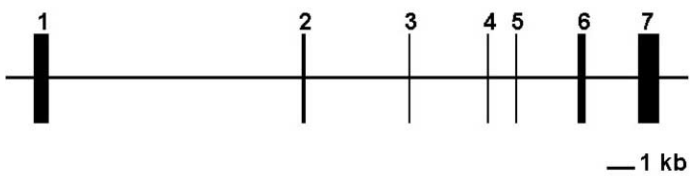

(B) Mouse *Gclm* gene structure

Exon	kb	Intron	kb
1	0.435	1	~9.5
2	0.126	2	~3.8
3	0.066	3	~2.8
4	0.085	4	0.9
5	0.060	5	~2.2
6	0.203	6	~1.4
7	0.721		
Total	1.696		20.6

Intron/Exon boundaries (exonic region in capital letters)

Boundary	Sequence
Exon 1/Intron 1	ACGCACAGCGAGGAGgtgagcacggtgggggccgagggtctcctc
Intron 1/Exon 2	tgataactttgaaaatgcttctttttgcagCTTCGGGACTGTATC
Exon 2/Intron 2	CCCGATTTAGTCAGGgtaagtagatgtgaatgcagaaaccctgca
Intron 2/Exon 3	tatgttcattgtatgttgtgtttcctgcagGAGTTTCCAGATGTT
Exon 3/Intron 3	AAATGAAAGTTTCTGgtaagctccgctctttttttctttttttt
Intron 3/Exon 4	acgcagtaaccaggtCttttcgttttccagCAAAACTGTTCATTG
Exon 4/Intron 4	GTGCAGTTGACATGGgtaagcagaaatttatttttcataataat
Intron 4/Exon 5	ttagccttttgtgtcttcctttccttcagCATGCTCCGTCCTTG
Exon 5/Intron 5	TATCAGTGGGCACAGgtaaagcacgtccggaccctgacacttgcg
Intron 5/Exon 6	gaatacagttcactttgtttccacttttagGTAAAACCCAATAGT
Exon 6/Intron 6	ACAATGACCCGAAAGgtgagactggcattttcatctctaggcttg
Intron 6/Exon 7	tcaaacctaacctgtgtggtgttgttttagAACTGCTCTCTGAGG
Exon 7/Poly A	AGTAATGTA**AATAAA**ATTCATTCTTTGATC

Fig. 5. The mouse *Gclm* gene structure (A), lengths (kb) of all exons and introns, and sequence analysis of the intron/exon junctions (B). Thirty base pairs of intronic sequence are included at both the donor and acceptor splice-site junctions. The consensus polyadelynation signal is bolded and underlined in (B).

taken in order to eliminate any possible artifacts that might result in truncated products possibly due to any DNA sequence variation between the different inbred strains of mice (cDNA in Hepa-1 cultures, derived from the C57L inbred mouse strain [29] vs. 129/SVJ genomic DNA).

Next, we performed RNase titration experiments, in order to rule out the possibility that overdigestion might result in the formation of truncated products. As shown in Fig. 6B, increasing the RNase concentration in our digestions refined the map of initiated products but did not generate truncated products. The protected fragments from 129/SVJ hepatic RNA and from Hepa-1 RNA were similar in size, suggesting that any sequence differences between these mouse strains do not contribute to differences in the start sites of transcription. Using yeast tRNA as a negative control, we failed to detect any protected products when it was incubated with the riboprobes. In addition, when RNA from induced cells was mixed with RNA from controls, the relative levels of detected products were always correlated with that of GCLM mRNA detected *via* RNA blot hybridization analysis (data not shown).

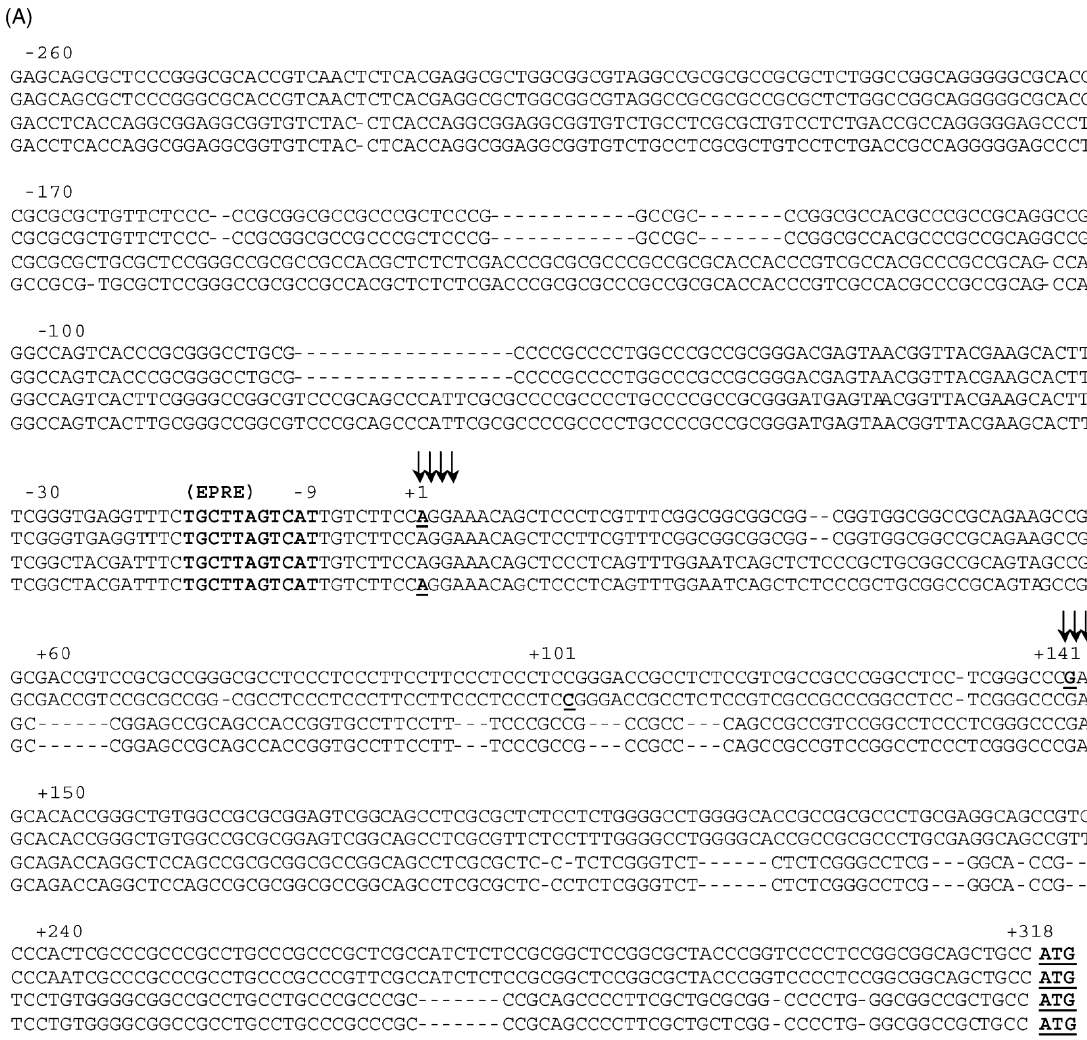

Fig. 6. (A) Alignment of the 584-bp sequence of the mouse *Gclm* gene from two laboratories and the human *GCLM* gene from two laboratories. (Row 1) The present study, (Row 2) [17], (Row 3) [15], and (Row 4) [16]. The numbering system starts as +1 for the first purine of the 5′-most transcription start-site of our mouse gene, and the next base upstream is −1 in the promoter. The putative functional inverted EPRE core sequence, starting at −9, is in bold. The transcription start-site clusters I and II are shown with arrows. The +1 adenine in our study and one human study [16] is underlined and in bold. The +101 cytosine in the other mouse study [17] is underlined and in bold. The +141 guanine at the beginning of cluster II in our study is underlined and in bold. The adenine at the translation start codon is +318. (B) RNase protection analysis of the GCLM mRNA. Ten milligrams of yeast tRNA (lane 1) or total RNA isolated from the livers of diethylmaleate-treated 129/SVJ mice (lane 2) or from tBHQ-treated Hepa-1 cells (lane 3) was denatured and hybridized with an antisense ^{32}P-labeled RNA probe encompassing nucleotides −224 to +298 of the *Gclm* 5′-flanking region and 5′-untranslated region (see (A)). Following hybridization, samples were digested with (A) 4.5, (B) 1.5, or (C) 0.5 mg RNase A—each containing 24 Egami U of RNAse T1. Following digestion, the samples were loaded on sequencing gels, and sizes of the protected transcripts were determined by comparison with a DNA-sequencing ladder and normalized with RNA standards (280- and 155-bp markers denoted by *arrows*). The two main transcription start-site clusters are indicated. All three probe products showed similar results, although only the results from the *Sac* II–*Blp* I probe are shown.

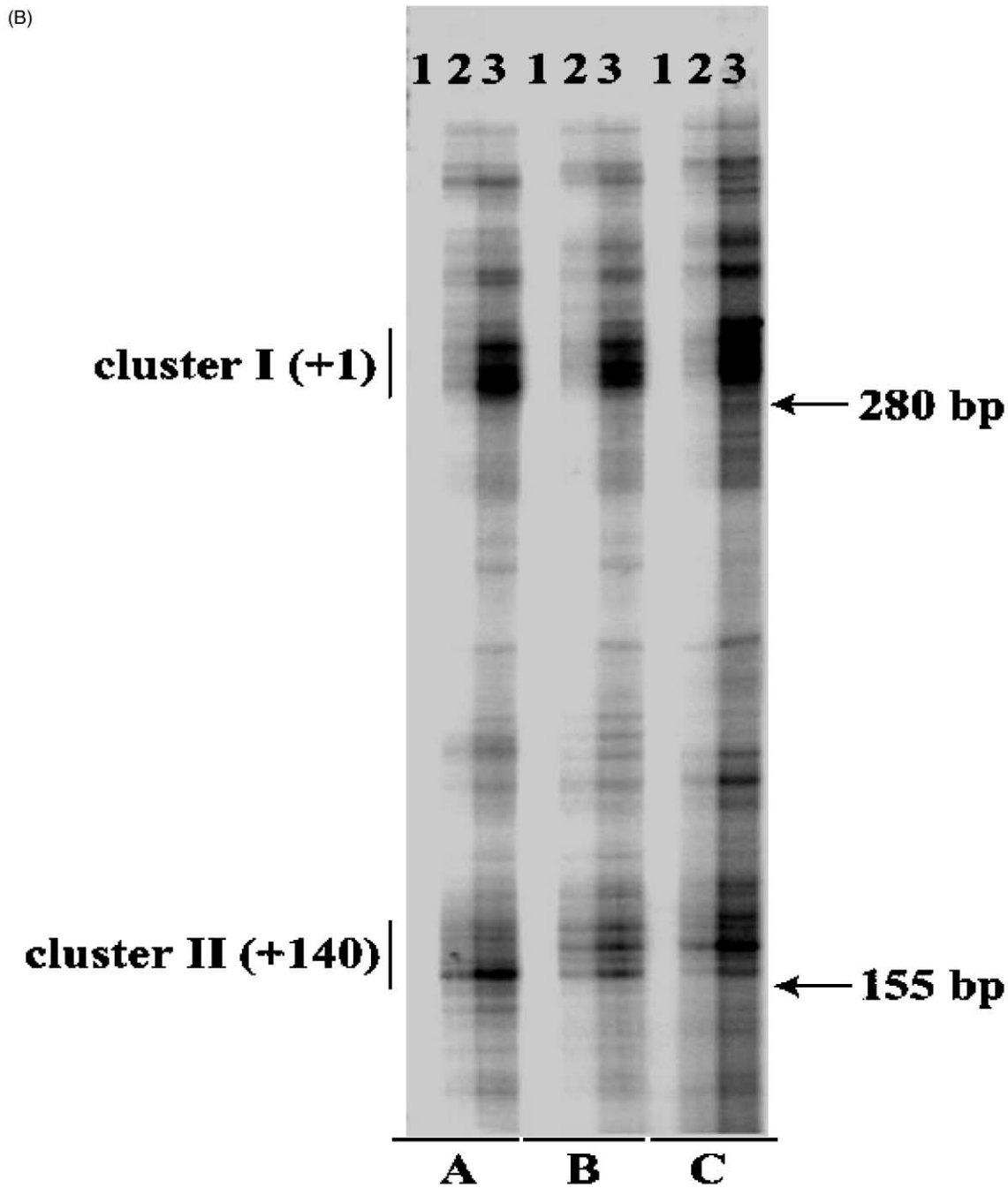

Fig. 6. (*Continued*).

RNase analysis thus uncovered two clusters of prominent transcriptional start-sites in the *Gclm* gene (Fig. 6), which map to 317 bp (cluster I) and 177 bp (cluster II) 5′-ward of the ATG translation initiation codon and account for approximately 55 and 30%, respectively, of the total GCLM transcripts, as determined by phosphorimager analysis. Following conventional nomenclature for genes with multiple start-sites, we have named the 5′-most base (an adenine) in the 5′-most transcription start-site cluster as "+1," and the first upstream base (a cytosine) as "−1" of the promoter region. The RNase analysis thus assigns the adenine in the ATG translation initiation codon as "+318" and the 3′ beginning of the putative EPRE as "−9" in the proximal promoter (Fig. 6A).

3.7. Characterization of the Gclm promoter

We sequenced 4.7 kb of the *Gclm* promoter and 5′-untranslated region; only 264 bp 5′-ward and 320 bp 3′-ward of the cluster I transcription start-sites are depicted in Fig. 6A, showing no TATA box motif, plus the GC-rich 5′-untranslated region and proximal promoter.

To determine *cis*-acting sequences responsible for the transcriptional induction of *Gclm*, we created a series of deletion constructs that included 4.7–0.5 kb of 5′-flanking sequence, including the cluster I and II transcription start-sites. These *Gclm* genomic fragments were found to drive expression of the firefly luciferase (*LUC*) reporter gene in transient transfections and were normalized for efficiency by co-transfecting a constitutively expressed β-galactosidase reporter construct. Initial experiments revealed that the basal activity of all *Gclm* 5′-flanking constructs (from 4.7 kb upstream, down to only 0.5 kb remaining) was much higher than that of the SV40 promoter controlling *LUC* expression (data not shown). In order to achieve maximal inducibility, we had to titrate down the promoter construct DNA concentration, while maintaining the total DNA concentration constant.

Constructs containing between 4.7 and 0.5 kb of the *Gclm* 5′-flanking region plus 5′-untranslated region (Fig. 7A) revealed only ∼2-fold increases in tBHQ-induced LUC activity. For the construct in which cluster I in the proximal promoter was deleted (Fig. 7B), induction was completely absent, and almost all (96%) of the basal LUC activity was lost. Interestingly, omission of cluster II, as demonstrated with the *0.5(Δ184)GclmLUC* construct, also lowered basal activity (to 12% of that seen with *0.5GclmLUC*) but did not affect the ∼2-fold induction by tBHQ. It should be noted that, despite these large decreases in basal LUC activities for these constructs, their levels are still at least 20-fold higher than that found with the transfected promoterless luciferase vector, PGL3 Basic (Fig. 7B). These data suggest that both clusters of transcriptional start sites are functional.

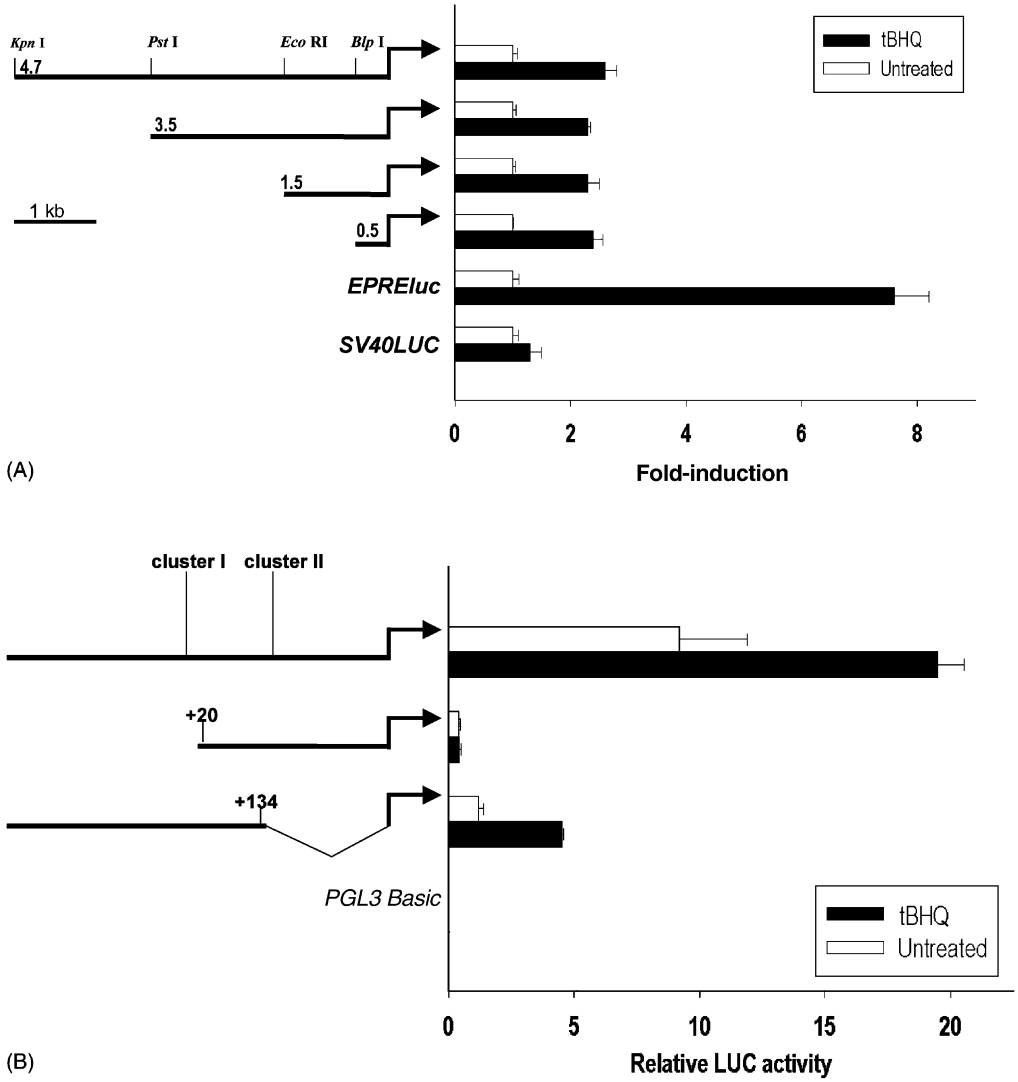

Fig. 7. Analysis of 4.7 kb of the mouse *Gclm* 5′-flanking region driving the *LUC* reporter gene. The LUC activity of four 5′-flanking segments are compared with the positive control *EPREluc* and the negative control *SV40LUC* constructs in (A). Deletion of transcription start-site cluster I, or deletion of start-site cluster II, is compared with the *0.5GclmLUC* and the negative control *PGL3 Basic* constructs in (B). Untreated transfected cells received the vehicle (DMSO) alone. Treated transfected cells were given 50 μM tBHQ for 12 hr. The results shown are the means ± SD of at least three independent experiments.

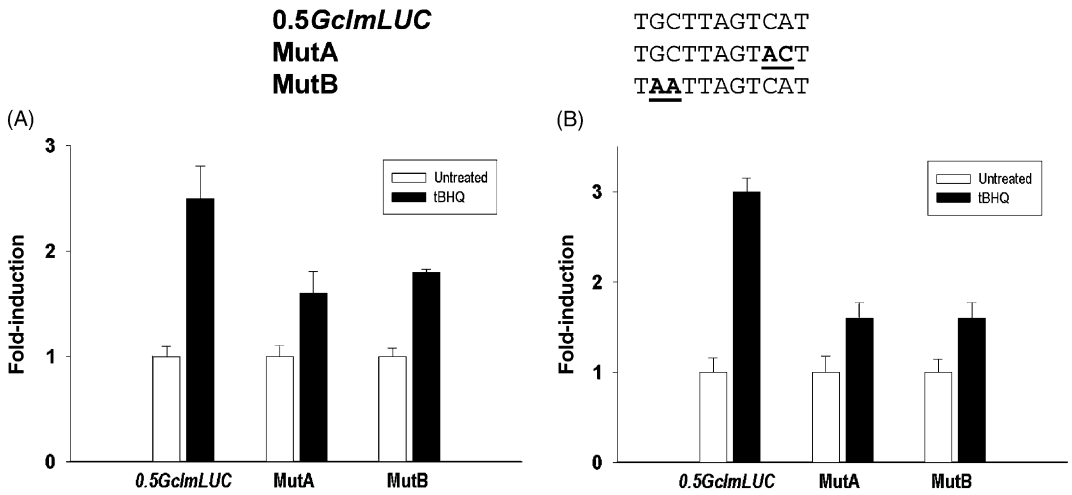

Fig. 8. Effects of the putative functional inverted EPRE core sequence following site-directed mutagenesis in two different locations.The constructs were transiently transfected (A) and stably transfected (B) into Hepa-1 cells, the cells were treated with tBHQ (50 μM) or vehicle only (DMSO) for 12 hr, and LUC activities were compared with that of the *0.5GclmLUC* control. MutA and MutB showed no differences from *0.5GclmLUC* in terms of basal LUC activity; thus, for the sake of simplicity, the fold-induction of LUC activity is shown. The results shown are the means ± SD for at least three independent experiments.

Induction from the responsive *Gclm* 5′-flanking constructs was lower than what might be expected, based on the robust transcriptional induction (6- to 7-fold) of the endogenous *Gclm* gene (Figs. 1–3). Lack of strong induction was not an artifact of our transfection system, however, because a single copy of the mouse glutathione *S*-transferase A1 (*Gsta1*) EPRE motif, driving luciferase (*i.e.* the *EPREluc* construct), responded with a 7- to 8-fold induction in parallel transfections (Fig. 7A). In untreated cell cultures, GCLM mRNA is generally maintained at relatively low levels, as compared with numerous other mRNAs; hence, the high basal activity of the *Gclm* reporter constructs and the low inducibility (Fig. 7) are both inconsistent with that seen for the endogenous gene in cultured cells.

3.8. Analysis of the −9 EPRE motif in the Gclm promoter

An inverted putative functional EPRE has been found in the human *GCLM* [15,16], mouse *Gclm* [17], and rat [18] promoters and has been suggested to play an important role in oxidative stress-induced up-regulation of the *GCLM* gene. These results are controversial, however, because one research group has found this EPRE to be irrelevant for *GCLM* inducibility under similar assay conditions [28].

To determine the function of this −9 EPRE in the mouse *Gclm* 5′-flanking region, we introduced mutated bases into the EPRE core motif. When the mutant constructs MutA and MutB were transiently transfected into Hepa-1 cells (Fig. 8), induction of LUC activity by tBHQ decreased approximately to 30%, as compared with that for the wild-type *0.5GclmLUC*.

To test the possibility that a robust transcriptional response from the *Gclm* 5′-flanking region may require chromatin structure, we generated pools of stable transfectants with several of our reporter constructs. Pools generated when our longest construct (4.7 kb of 5′-flanking sequence) was used exhibited a similar fold-induction to pools generated when our *0.5GclmLUC* was used (data not

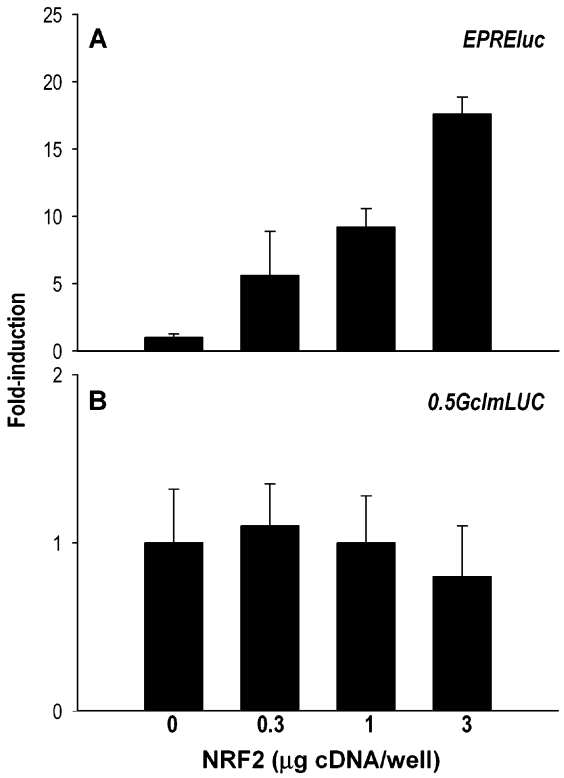

Fig. 9. Effects of increasing concentrations of NRF2 cDNA (μg per well) on LUC activity of the transiently transfected *EPREluc* positive control (A) and the *0.5GclmLUC* construct (B) containing the −9 EPRE core sequence. Results are shown as fold-induction means ± SD for at least three independent experiments. Note the large differences in scale on the ordinate between (A) and (B).

shown). tBHQ-mediated LUC induction in these stable transfectants was not appreciably increased, compared with that in transient transfections. We also compared pools of stable transfectants containing the MutA and MutB constructs with *0.5GclmLUC* (Fig. 8). tBHQ-mediated LUC induction of both constructs containing mutant EPRE sequences were diminished by approximately 50%, as compared with *0.5GclmLUC* showing no decrease in basal LUC activity. Our results with stable transfectants are thus entirely consistent with those derived from transient transfection analysis.

Previous work has specifically implicated the bZIP transcription factor NRF2 in transactivation of the −9 EPRE motif in the human *GCLM* promoter [27]. To assess the degree of function of this EPRE in the mouse *Gclm* gene, we co-transfected either the the *EPREluc* or the *0.5GclmLUC* reporter gene construct in the presence of increasing concentrations of a plasmid expressing NRF2 (Fig. 9). The results show that increases in NRF2 concentrations are able to enhance LUC activity in a dose-dependent manner for the *EPREluc* positive control, but not at all for the *0.5GclmLUC* construct. It might be noted that the small MAF homodimers and some heterodimers can bind to EPRE motifs independently of NRF2—if the EPRE sequence resembles the MAF recognition element (MARE)—but that such MAF homodimers act as transcriptional repressors [51].

4. Discussion

In this study, we have examined GCLM and GCLC mRNA accumulation, following induction by tBHQ in mouse Hepa-1 cells, and have determined that the mechanism of increase is mostly transcriptional. In addition, we observed that strikingly lowered GSH levels do not cause *Gclm* or *Gclc* up-regulation. We also find that the robust induction of the *Gclm* gene in Hepa-1 cells is much greater than the *Gclm* 5′-flanking region-driven reporter constructs transiently or stably transfected. In the 4.7 kb of the *Gclm* 5′-flanking region that we sequenced, the only pro-oxidant-responsive motif was an inverted EPRE located 9 bp upstream of the 5′-most transcription start-site. Although this −9 EPRE appears partially responsible for tBHQ-mediated induction, the major enhancer of *Gclm* up-regulation by oxidative stress may be further 5′-ward, intronic, or 3′-ward of the 4.7 kb of 5′-flanking region studied in our experiments.

4.1. Increases primarily in transcription

In the present study, comparing hydrogen peroxide, menadione, cadmium and arsenite with tBHQ, we found tBHQ to be the best inducer for *Gclm* and *Gclc* in Hepa-1 cells (Figs. 1 and 2), and we have shown that this response is largely at the transcriptional level (Fig. 3). *Gclm* induction was far more robust compared to *Gclc*, implying that the levels of GCLM may have the more dominant role in modulating the intracellular GSH levels. Oxidative stress is commonly associated with GSH depletion, and GSH is known to be a feedback inhibitor of GCL activity [1–3,49]. Surprisingly, when we depleted GSH and increased the GS–SG/GSH ratio with BSO, no differences in GCLC or GCLM mRNA levels were observed (Fig. 4). Liver cells have high GSH concentrations—possibly compartmentalized between the cytosol, nucleus and mitochondria—which might have been able to compensate for BSO-induced GSH depletion.

Another group has shown a similar trend in rat cells treated with a product of lipid peroxidation as their inducer [14]. Their results demonstrated a transcriptional increase for both *GCLC* and *GCLM* genes, with a more pronounced induction for *GCLM*, in agreement with what was found in the present study. In addition to showing that this response occurs at the transcriptional level, they also reported an increase in mRNA stability for both genes [14]; in contrast, we found no detectable differences in mRNA stability for either the *Gclc* or *Gclm* gene. These discrepancies might be due to the different oxidative stress inducer and/or the different cell lines used.

4.2. Location of transcription start-sites

In the present study, RNase protection analysis was used to identify the transcriptional start-sites of the *Gclm* gene. Consistent with the *Gclm* 5′-flanking region being both GC-rich and without a TATA box, we mapped multiple major and minor transcriptional start-sites (Fig. 6). As discussed below, multiple transcriptional start-sites are commonly associated with TATA-less promoters. For several reasons, we believe that our analysis documents the accurate start-sites of the mouse *Gclm* gene. First, no protected products were observed when we used an equal quantity of tRNA. Second, the pattern of protected products was essentially identical (although the relative abundance of protected fragments differed to some degree) between RNA isolated from Hepa-1 cells or 129/SVJ mouse liver RNA. Our RNase protection probes were derived from DNA isolated from 129/SVJ mice. Third, the level of protected fragments was always correlated with the level of GCLM mRNA. This is apparent when comparing the relative abundance of protected products from tBHQ-induced Hepa-1 cells with that from diethylmaleate-induced 129/SVJ mouse liver (i.e. Hepa-1 cells accumulated considerably more GCLM transcript than 129/SVJ mouse liver; results of RNA hybridization analysis not shown).

Although our methodologies differ, sequence alignment demonstrates that we identify the same major start-site for transcription from cluster I as Galloway *et al.* [16] did for the human *GCLM* gene. This group also identified several minor start-sites adjacent to cluster I. On the other hand, using primer extension, Hudson and Kavanagh [17]

identified a single transcriptional start site for mouse *Gclm* at position +101 relative to cluster I. The reason for this discrepancy is unclear. It should be noted that the position of the primer used for extension in their study [17] was very near to cluster II, so that the small extended fragments may not have been detected in their primer extension assay. In addition, it is not possible to speculate whether primer extension analysis used by Galloway *et al.* [16] would have detected initiation from cluster II, because they report using a primer encompassing nucleotides –266 to –427, (161 bases), which is apparently a mis-statement.

Overall the sites of transcriptional initiation mapped in the present study are supported teleologically and experimentally by three observations: (a) the transcriptional initiation sites map to regions of the *Gclm* 5′-flanking region that are highly conserved between mouse and human (Fig. 6A). Sequence conservation in 5′-flanking regions between species as divergent as mouse and human is generally maintained when the same DNA regions are used for the binding of regulatory proteins such as those responsible for transcriptional initiation; (b) transcriptional initiation maps to multiple start-sites, as is common with GC-rich TATA-less promoters. Moinova and Mulcahy [15] described multiple start-sites for the human *GCLM* gene, although they did not present the data; (c) our transient transfection analysis demonstrates considerable basal activity, using constructs that contain only cluster I or II (Fig. 7B). These findings suggest that both of these DNA regions support transcriptional initiation.

4.3. Mammalian GCLM, a TATA-less gene

We and others have found no canonical TATA box for *GCLM* gene, and the transcription start-site clusters are located in a GC-rich region. Thus, the mouse *Gclm* 5′-flanking region resembles that of other "housekeeping genes" that are expressed constitutively [31]. Quite remarkably, and in contrast to most housekeeping genes, however, the mammalian *GCLM* gene can be highly induced by environmental signals, such as oxidant stressors.

Regulation of TATA-less promoters appears to be complex [52]; transcription is commonly initiated at multiple sites, and DNA sequences—termed initiator (INR) regions—are involved in directing transcription [53]. In TATA-less promoters, INRs contain a "loose" DNA consensus that has been shown to interact with the basal transcription machinery, determine the start of transcription, and authorize the direction of transcription [52–55]. Another salient characteristic of the TATA-less promoter is the presence of numerous SP1-binding sites. SP1 transcription factors have been demonstrated to interact with proteins that bind to INRs and which contribute to the tissue- and cell type-specific regulation of their target genes [56,57]. There are numerous putative SP1-binding sites (e.g. CCCGCC) in the 5′-untranslated region and proximal promoter shown in Fig. 6A.

4.4. Search of the mouse Gclm 5′-flanking region for oxidative stress-induced regulation

Analysis of the mouse *Gclm* 5′-flanking region, from the transcription start-sites up to −4.7 kb (Fig. 7), showed high basal expression, yet disappointingly small induction by tBHQ. Consistent with these data, analysis of the DNA sequence gave no candidate other than the −9 EPRE. The results of the 5′-flanking constructs did not parallel the strong inducibility of the endogenous gene, nor the low basal activity, as observed by Northern blot (Figs. 1 and 2) and nuclear run-on (Fig. 3) analysis in the intact Hepa-1 cells.

Not surprisingly, analysis of the *Gclm* 5′-flanking region (Fig. 7) does show that the basal transcriptional machinery is affected considerably by the presence of cluster II, and especially cluster I, transcription start-sites. We did not examine *Gclm* 5′-flanking function in the presence of only cluster I in the absence of the putative functional inverted EPRE, and *vice versa*, and perhaps this should be done; however, only nine bases separate these two.

4.5. The EPRE motif

There are differences in opinion as to what exactly constitutes a functional EPRE. On one hand, there is the 10-bp EPRE "core," GTGACnnnGC (n = any nucleotide), as described in the promoters for the rat *GSTA1* and *NQO1* genes [58], which are functionally essential for the response to electrophiles in the context of the endogenous 5′-flanking regions of these genes. On the other hand, there appears to be an "extended" EPRE motif in which additional bases flanking the GTGACnnnGC have been shown to be critical for function in the context of a minimal promoter; without such additional flanking bases, the core motif remains nonfunctional [59]. Following these criteria, the −9 EPRE in the mouse *Gclm* and human *GCLM* promoters can be seen to match only the EPRE core and not the extended EPRE motif. Moreover, the proteins that bind to the EPRE motif have not been fully characterized, thus adding further to the complexity about the mechanism of EPRE-mediated up-regulation.

Mutations in critical bases of the EPRE core (Fig. 8) produced small decreases in tBHQ inducibility, but no effects on basal *Gclm* promoter activity. By increasing concentrations of NRF2 expression (Fig. 9), we saw enhanced LUC activity using the *EPREluc* construct, but this had no effect on the *0.5GclmLUC* construct. We, therefore, conclude that, consistent with the view that the EPRE flanking sequences are critical to function [59], the −9 EPRE in the mouse *Gclm* gene, not having these flanking sequences, contributes very little to the oxidative stress-induced up-regulation of this gene.

In this report, we have characterized the magnitude of the transcriptional response of the *Gclm* gene to the strong inducer, tBHQ. As noted above, GCLM mRNA may be

regulated at the transcriptional and post-transcriptional levels. Thus, we considered it extremely important to document the relative level of transcriptional response in Hepa-1 cells, which we would eventually use to perform promoter analysis. In tBHQ-treated Hepa-1 cells, the accumulation of GCLM mRNA is primarily, if not entirely, the result of a robust increase in transcription. This result suggests that Hepa-1 would be an excellent cell line in which to delineate the 5′-flanking elements that drive *Gclm* transcriptional responses. Next, it was essential to define the transcriptional start-site(s) for this gene, because these sites must be included in constructs that analyze 5′-flanking region and promoter function. Our constructs included both of two regions that demonstrate a high degree of homology between the mouse *Gclm* and human *GCLM* genes and were shown by RNase protection and transient transfection in the present study to be sites of transcriptional initiation. A LUC-reporter construct containing this proximal promoter and 4.7 kb of 5′-flanking region was tested, and LUC activity was found to accumulate in response to tBHQ. The results of this 5′-flanking analysis, even though our constructs contained the most proximal transcriptional start-sites, are consistent with other reports of weak (2-fold) transcriptional inductions supported by the *Gclm* promoter and limited 5′-flanking sequence.

Do these sequences contain the response elements responsible for the robust transcriptional induction of the *Gclm* gene? While we acknowledge that the magnitude of transcriptional response in reporter gene analysis need not correlate in magnitude with the transcriptional response of the endogenous gene, additional pieces of evidence suggest that our constructs, and those of others in the field, lack important regulatory elements that may be responsible for the enhanced transcriptional response. First, in our system a single extended EPRE cloned behind a minimal promoter does respond robustly when cells are treated with tBHQ. Second, the basal activity of our constructs is extremely high. Does this suggest that elements outside the proximal promoter decrease promoter occupancy and lower the basal expression of the endogenous gene? If so, we have yet to locate these control elements. Third, the inducible activity of our 5′-flanking constructs does not increase when these constructs are stably transfected into cells. If the *Gclm* 5′-flanking region needs to be packaged into chromatin for proper regulation, then induction should have been increased in stably expressing cells. Taken together, we believe our results leave doubt that any motif included in –4.7 kb of the mouse *Gclm* promoter contains the most powerful regulatory elements that support induction of the *Gclm* gene.

We believe that further analysis—of sequences 5′-ward or 3′-ward of the sequence that we studied—is warranted. It is not uncommon to find regulatory elements within intronic sequences that have marked effects on gene expression [60–62]. In this regard, we have analyzed the 5′-most 7 kb of the intron 1 of the *Gclm* gene for enhancer activity. This sequence had no effect on basal activity or tBHQ inducibility from the *0.5GclmLUC* construct (data not shown). Perhaps control elements are located further 5′-ward of the –4.7 kb construct reported herein. Interestingly, as an example, although some regulatory elements were located within the first 4 kb of the mouse *Hmox1* promoter, a strong EPRE enhancer was subsequently localized about 10 kb upstream [63].

5. Conclusions

In summary, we found robust transcriptional induction and mRNA accumulation for the endogenous *Gclm* gene in mouse Hepa-1 cells by treatment with tBHQ and four other agents that cause oxidative stress. We do not see such a robust effect, however, in 4.7 kb of the *Gclm* 5′-flanking region driving the reporter gene, in transient as well as stable transfections. Deletion analysis of this 5′-flanking region has shown that sequences surrounding transcription start-site cluster I are important for basal activity and, perhaps in small part, for tBHQ inducibility. It seems highly likely that the −9 EPRE is necessary but not sufficient in that it does not represent the major enhancer response element stimulated by oxidative stress, although it is located within the complex promoter of a TATA-less gene. Careful *in vivo* footprinting of the region between −30 and +210 (Fig. 6A), which contains this EPRE and the two transcription start-site clusters, is needed to understand better the constitutive regulation of this gene. More sequencing—5′-ward of the 4.7 kb examined in the present study, sequencing of all introns, and perhaps 3′-ward of the last exon—will be necessary in order to locate the major enhancer(s) and transcription factors involved in *Gclm* upregulation by oxidative stress.

Acknowledgments

These data were presented, in large part, at the 20th Annual Meeting of the Society of Toxicology in Philadelphia [*The Toxicologist* 54: abstract #1188 (March, 2000)]. We thank our colleagues for valuable discussions and a careful reading of this manuscript. We are very grateful to J.Y. Chan, Ph.D. (Department of Laboratory Medicine, University of California, San Francisco) for providing us with the NRF2 cDNA expression vector. This work was partially funded by National Institutes of Health (NIH) Grants R01 AG09235, R01 ES10416, and P30 ES06096.

Note added in proof

Alignment of the 584 bases (depicted in Fig. 6A) between the mouse *Gclm* and human *GCLM* 5′-flanking regions shows 75.7% nucleotide identity. Because the mouse–rat split occurred in evolution about one-fourth

as long ago as mouse–human divergence [64], we would, therefore, expect the mouse–rat alignment to show about 94% nucleotide identity. After submitting our manuscript, the rat *GCLM* 5′-flanking sequence was reported [18]. Yang *et al*. found no EPRE, but 12 (!) AP1 sites, in 1.86 kb of 5′-flanking region sequenced, and they found only a 177- and a 46-bp region of the rat having 94 and 93% nucleotide identity, respectively, to regions of the mouse *Gclm* 5′-untranslated region (these two segments correspond to +51 to +227 and +272 to +318, using our numbering in Fig. 6A). However, overall alignment of the 584 bases in Fig. 6A between rat and mouse gives only 59% identity—when ∼94% identity would be expected. This discrepancy can be explained either by more than one insertion or deletion of DNA in the rat *GCLM* 5′-flanking region during the past 17 million years, or by Yang *et al*. [18] having inadvertently cloned a GC-rich 5′-flanking region of another gene.

References

[1] Meister A. Glutathione metabolism. Meth Enzymol 1995;251:3–7.

[2] Anderson ME. Glutathione: an overview of biosynthesis and modulation. Chem-Biol Interact 1998;111–112:1–14.

[3] Lu SC. Regulation of hepatic glutathione synthesis: current concepts and controversies. FASEB J 1999;13:1169–83.

[4] Huang CS, Anderson ME, Meister A. Amino acid sequence and function of the light subunit of rat kidney γ-glutamylcysteine synthetase. J Biol Chem 1993;268:20578–83.

[5] Wild AC, Mulcahy RT. Regulation of γ-glutamylcysteine synthetase subunit gene expression: insights into transcriptional control of antioxidant defenses. Free Radic Res 2000;32:281–301.

[6] Griffith OW, Mulcahy RT. The enzymes of glutathione synthesis: γ-glutamylcysteine synthetase. Adv Enzymol Relat Areas Mol Biol 1999;73:209–67.

[7] Mulcahy RT, Gipp JJ. Identification of a putative antioxidant response element in the 5′-flanking region of the human γ-glutamylcysteine synthetase heavy subunit gene. Biochem Biophys Res Commun 1995;209:227–33.

[8] Mulcahy RT, Wartman MA, Bailey HH, Gipp JJ. Constitutive and β-naphthoflavone-induced expression of the human γ-glutamylcysteine synthetase heavy subunit gene is regulated by a distal antioxidant response element/TRE sequence. J Biol Chem 1997;272:7445–54.

[9] Wild AC, Gipp JJ, Mulcahy RT. Overlapping antioxidant response element and PMA response element sequences mediate basal and β-naphthoflavone-induced expression of the human γ-glutamylcysteine synthetase catalytic subunit gene. Biochem J 1998;332:373–81.

[10] Rahman I, Smith CA, Antonicelli F, MacNee W. Characterisation of γ-glutamylcysteine synthetase-heavy subunit promoter: a critical role for AP-1. FEBS Lett 1998;427:129–33.

[11] Rahman I, Smith CA, Lawson MF, Harrison DJ, MacNee W. Induction of γ-glutamylcysteine synthetase by cigarette smoke is associated with AP-1 in human alveolar epithelial cells. FEBS Lett 1996;396:21–5.

[12] Iwanaga M, Mori K, Iida T, Urata Y, Matsuo T, Yasunaga A, Shibata S, Kondo T. Nuclear factor κB-dependent induction of γ-glutamylcysteine synthetase by ionizing radiation in T98G human glioblastoma cells. Free Radic Biol Med 1998;24:1256–68.

[13] Lu SC, Huang ZZ, Yang JM, Tsukamoto H. Effect of ethanol and high-fat feeding on hepatic γ-glutamylcysteine synthetase subunit expression in the rat. Hepatology 1999;30:209–14.

[14] Liu RM, Gao L, Choi J, Forman HJ. γ-glutamylcysteine synthetase: mRNA stabilization and independent subunit transcription by 4-hydroxy-2-nonenal. Am J Physiol 1998;275:L861–9.

[15] Moinova HR, Mulcahy RT. An electrophile responsive element (EPRE) regulates β-naphthoflavone induction of the human γ-glutamylcysteine synthetase regulatory subunit gene. Constitutive expression is mediated by an adjacent AP-1 site. J Biol Chem 1998;273:14683–9.

[16] Galloway DC, Blake DG, McLellan LI. Regulation of γ-glutamylcysteine synthetase regulatory subunit (*GLCLR*) gene expression: identification of the major transcriptional start site in HT29 cells. Biochim Biophys Acta 1999;1446:47–56.

[17] Hudson FN, Kavanagh TJ. Cloning and characterization of the proximal promoter region of the mouse glutamate-L-cysteine ligase regulatory subunit gene. Biochim Biophys Acta 2000;1492:447–51.

[18] Yang H, Wang J, Ou X, Huang ZZ, Lu SC. Cloning and analysis of the rat glutamate-cysteine ligase modifier subunit promoter. Biochem Biophys Res Commun 2001;285:476–82.

[19] Favreau LV, Pickett CB. The antioxidant response element. In: Forman HJ, Cadenas E, editors. New York: Chapman & Hall; 1997. p. 272–87.

[20] Jaiswal AK. Antioxidant response element. Biochem Pharmacol 1994;48:439–44.

[21] Chan K, Lu R, Chang JC, Kan YW. NRF2, a member of the NFE2 family of transcription factors, is not essential for murine erythropoiesis, growth, or development. Proc Natl Acad Sci USA 1996;93:13943–8.

[22] Hayes JD, Chanas SA, Henderson CJ, McMahon M, Sun C, Moffat GJ, Wolf CR, Yamamoto M. The NRF2 transcription factor contributes both to the basal expression of glutathione *S*-transferases in mouse liver and to their induction by the chemopreventive synthetic antioxidants, butylated hydroxyanisole and ethoxyquin. Biochem Soc Trans 2000;28:33–41.

[23] Ishii T, Itoh K, Takahashi S, Sato H, Yanagawa T, Katoh Y, Bannai S, Yamamoto M. Transcription factor NRF2 coordinately regulates a group of oxidative stress-inducible genes in macrophages. J Biol Chem 2000;275:16023–9.

[24] Enomoto A, Itoh K, Nagayoshi E, Haruta J, Kimura T, O'Connor T, Harada T, Yamamoto M. High sensitivity of *Nrf2* knockout mice to acetaminophen hepatotoxicity associated with decreased expression of ARE-regulated drug-metabolizing enzymes and antioxidant genes. Toxicol Sci 2001;59:169–77.

[25] Chan K, Kan YW. NRF2 is essential for protection against acute pulmonary injury in mice. Proc Natl Acad Sci USA 1999;96:12731–6.

[26] Chan K, Han XD, Kan YW. An important function of NRF2 in combating oxidative stress: detoxification of acetaminophen. Proc Natl Acad Sci USA 2001;98:4611–6.

[27] Wild AC, Moinova HR, Mulcahy RT. Regulation of γ-glutamylcysteine synthetase subunit gene expression by the transcription factor NRF2. J Biol Chem 1999;274:33627–36.

[28] Galloway DC, McLellan LI. Inducible expression of the γ-glutamylcysteine synthetase light subunit by *tert*-butylhydroquinone in HepG2 cells is not dependent on an antioxidant-responsive element. Biochem J 1998;336:535–9.

[29] Darlington GJ, Bernhard HP, Miller RA, Ruddle FH. Expression of liver phenotypes in cultured mouse hepatoma cells. J Natl Cancer Inst 1980;64:809–19.

[30] Bauman JW, Liu YP, Andrews GK, Klaassen CD. Examination of potential mechanism(s) of metallothionein induction by diethylmaleate. Toxicol Appl Pharmacol 1992;117:226–32.

[31] Melton DW, Konecki DS, Brennand J, Caskey CT. Structure, expression, and mutation of the hypoxanthine phosphoribosyltransferase gene. Proc Natl Acad Sci USA 1984;81:2147–51.

[32] Dalton T, Palmiter RD, Andrews GK. Transcriptional induction of the mouse metallothionein-I gene in hydrogen peroxide-treated Hepa cells involves a composite major late transcription factor/antioxidant

response element and metal response promoter elements. Nucleic Acids Res 1994;22:5016–23.
[33] Dalton T, Pazdernik TL, Wagner J, Samson F, Andrews GK. Temporalspatial patterns of expression of metallothionein-I and -III and other stress-related genes in rat brain after kainic acid-induced seizures. Neurochem Int 1995;27:59–71.
[34] Vasiliou V, Theurer MJ, Puga A, Reuter SF, Nebert DW. Mouse dioxin-inducible NAD(P)H:menadione oxidoreductase: NMO1 cDNA sequence and genetic differences in mRNA levels. Pharmacogenetics 1994;4:341–8.
[35] Maier A, Dalton TP, Puga A. Disruption of dioxin-inducible phase I and phase II gene expression patterns by cadmium, chromium, and arsenic. Mol Carcinog 2000;28:225–35.
[36] Chomczynski P, Sacchi N. Single-step method of RNA isolation by acid guanidinium thiocyanate-phenol-chloroform extraction. Anal Biochem 1987;162:156–9.
[37] Dalton T, Kover K, Dey SK, Andrews GK. Analysis of the expression of growth factor, interleukin-1, and lactoferrin genes and the distribution of inflammatory leukocytes in the preimplantation mouse oviduct. Biol Reprod 1994;51:597–606.
[38] Krieg PA, Melton DA. Functional messenger RNAs are produced by SP6 *in vitro* transcription of cloned cDNAs. Nucleic Acids Res 1984;12:7057–70.
[39] Melton DA, Krieg PA, Rebagliati MR, Maniatis T, Zinn K, Green MR. Efficient *in vitro* synthesis of biologically active RNA and RNA hybridization probes from plasmids containing a bacteriophage SP6 promoter. Nucleic Acids Res 1984;12:7035–56.
[40] Zinn K, DiMaio D, Maniatis T. Identification of two distinct regulatory regions adjacent to the human β-interferon gene. Cell 1983;34:865–79.
[41] Reid LL, Botta D, Shao J, Hudson FN, Kavanagh TJ. Molecular cloning and sequencing of the cDNA encoding mouse glutamate-cysteine ligase regulatory subunit. Biochim Biophys Acta 1997;1353: 107–10.
[42] Prestera T, Holtzclaw WD, Zhang Y, Talalay P. Chemical and molecular regulation of enzymes that detoxify carcinogens. Proc Natl Acad Sci USA 1993;90:2965–9.
[43] Dieter MZ, Freshwater SL, Solis WA, Nebert DW, Dalton TP. Tyrphostin AG879, a tyrosine kinase inhibitor: prevention of transcriptional activation of the electrophile and aromatic hydrocarbon response elements. Biochem Pharmacol 2000;61:215–25.
[44] Chan JY, Kwong M. Impaired expression of glutathione synthetic enzyme genes in mice with targeted deletion of the NRF2 basic-leucine zipper protein. Biochim Biophys Acta 2000;1517:19–26.
[45] Alam J, Stewart D, Touchard C, Boinapally S, Choi AM, Cook JL. NRF2, a cap 'n' collar transcription factor, regulates induction of the heme oxygenase-1 gene. J Biol Chem 1999;274:26071–8.
[46] Chen C, Okayama H. High-efficiency transformation of mammalian cells by plasmid DNA. Mol Cell Biol 1987;7:2745–52.
[47] Senft AP, Dalton TP, Shertzer HG. Determining glutathione and glutathione disulfide using the fluorescence probe *o*-phthalaldehyde. Anal Biochem 2000;280:80–6.
[48] Vasiliou V, Buetler T, Eaton DL, Nebert DW. Comparison of oxidative stress response parameters in newborn mouse liver versus SV40-transformed hepatocyte cell lines. Biochem Pharmacol 2000; 59:703–12.
[49] Dalton TP, Shertzer HG, Puga A. Regulation of gene expression by reactive oxygen. Annu Rev Pharmacol Toxicol 1999;39:67–101.
[50] Shertzer HG, Vasiliou V, Liu RM, Tabor MW, Nebert DW. Enzyme induction by *L*-buthionine (*S*,*R*)-sulfoximine in cultured mouse hepatoma cells. Chem Res Toxicol 1995;8:431–6.
[51] Motohashi H, Shavit JA, Igarashi K, Yamamoto M, Engel JD. The world according to Maf. Nucleic Acids Res 1997;25:2953–9.
[52] Azizkhan JC, Jensen DE, Pierce AJ, Wade M. Transcription from TATA-less promoters: dihydrofolate reductase as a model. Crit Rev Eukaryot Gene Expr 1993;3:229–54.
[53] Smale ST, Baltimore D. The "initiator" as a transcription control element. Cell 1989;57:103–13.
[54] O'Shea-Greenfield A, Smale ST. Roles of TATA and initiator elements in determining the start-site location and direction of RNA polymerase II transcription. J Biol Chem 1992;267:1391–402.
[55] Javahery R, Khachi A, Lo K, Zenzie-Gregory B, Smale ST. DNA sequence requirements for transcriptional initiator activity in mammalian cells. Mol Cell Biol 1994;14:116–27.
[56] Smale ST, Schmidt MC, Berk AJ, Baltimore D. Transcriptional activation by SP1 as directed through TATA or initiator: specific requirement for mammalian transcription factor IID. Proc Natl Acad Sci USA 1990;87:4509–13.
[57] Lu J, Lee W, Jiang C, Keller EB. Start site selection by SP1 in the TATA-less human *Ha-ras* promoter. J Biol Chem 1994;269:5391–402.
[58] Rushmore TH, Morton MR, Pickett CB. The antioxidant responsive element. Activation by oxidative stress and identification of the DNA consensus sequence required for functional activity. J Biol Chem 1991;266:11632–9.
[59] Wasserman WW, Fahl WE. Functional antioxidant responsive elements. Proc Natl Acad Sci USA 1997;94:5361–6.
[60] Antoniou M, Geraghty F, Hurst J, Grosveld F. Efficient 3′-end formation of human β-globin mRNA *in vivo* requires sequences within the last intron but occurs independently of the splicing reaction. Nucleic Acids Res 1998;26:721–9.
[61] Wandersee NJ, Ferris RC, Ginder GD. Intronic and flanking sequences are required to silence enhancement of an embryonic β-type globin gene. Mol Cell Biol 1996;16:236–46.
[62] Vyas P, Vickers MA, Picketts DJ, Higgs DR. Conservation of position and sequence of a novel, widely expressed gene containing the major human α-globin regulatory element. Genomics 1995;29: 679–89.
[63] Hartsfield CL, Alam J, Choi AM. Transcriptional regulation of the heme oxygenase-1 gene by pyrrolidine dithiocarbamate. FASEB J 1998;12:1675–82.
[64] Nebert DW, Gonzalez FJ. P450 genes: Structure, evolution and regulation. Annu Rev Biochem 1987;56:945–93.